Water and Environment Journal
Promoting Sustainable Solutions
CIWEM

Water and Environment Journal. Print ISSN 1747-6585

Surface coating of polyamide reverse osmosis membranes with zwitterionic 3-(3,4-dihydroxyphenyl)-L-alanine (L-DOPA) for forward osmosis

Seda Saki[1] & Nigmet Uzal [2]

[1]Materials Science and Mechanical Engineering, Abdullah Gül University, Kayseri, Turkey and [2]Department of Civil Engineering, Abdullah Gül University, Kayseri, Turkey

Keywords
forward osmosis; L-DOPA; reverse osmosis; surface modification.

Correspondence
Nigmet Uzal, Department of Civil Engineering, Abdullah Gül University, Kayseri, 38080, Turkey.
Email: nigmet.uzal@agu.edu.tr

doi:10.1111/wej.12475

Abstract

To overcome low permeability and fouling problems of membranes used in FO processes, modification is needed to improve the hydrophilicity, permeability and selectivity of membranes. In this work, thin film composite (TFC) commercial polyamide RO membranes (BW30-LE, SW30-HR, AG and AC) were functionalized with zwitterionic L-DOPA. The effect of L-DOPA on the morphology of membranes was determined via SEM, FT-IR, AFM and contact angle analysis. The L-DOPA modified BW30-LE membrane showed excellent properties with 46° contact angle and 3.8 L/m^{2}hbar water permeability and 0.83 L/m^{2}h salt permeability. Although, L-DOPA modified BW30-LE membrane had the highest water flux and hydrophilicity, L-DOPA modified SW30-HR membrane showed higher FO flux with 9.38 L/m^{2}h than BW 30 membrane with 3.5 L/m^{2}h at 50 g/L NaCl draw solution. Introducing hydroxyl and carboxyl ionic groups on the membrane surface with L-DOPA coating enhanced the FO performance and water permeability which provide a new insight in FO applications.

Introduction

Compared to the pressure-driven membrane technologies, FO has attracted growing interest because of utilizing natural driving force generated by salinity gradient solutions with minimal energy input so as low capital and operational costs, lower fouling tendency, less pretreatment requirements and high rejection to salts and many contaminants (Chowdhury *et al*., 2017; Ge *et al.*, 2017; Tian *et al.*, 2017b). FO utilizes osmotic gradient as the driving force to transport water from feed solution to draw solution across a semi-permeable membrane (Shen and Wang, 2018). With the increasing attention on FO process in the last years (Tian *et al*., 2017a), it has become available for a wide range of potential applications, like as wastewater treatment (Lutchmiah *et al.*, 2014), seawater desalination (Boo *et al.*, 2013), power generation (Achilli *et al.*, 2009), liquid food processing (Wang *et al.*, 2017) and pharmaceutical rejection (Jin *et al.*, 2012).

Although, polyamide thin film composite (TFC) FO membranes have been extensively in use as a result of their higher selectivity and water flux performances, current FO membranes cannot meet the cost and performance requirements (Yang *et al.*, 2018; Xie *et al.*, 2018). Under this view; membrane fouling (Lee *et al.*, 2010; Ni and Ge, 2018), reverse solute diffusion (Hancock and Cath, 2009) and concentration polarization (CP) (Wang *et al.*, 2010a) are the drawbacks that challenge the application of FO membranes in water treatment (Goosen *et al.*, 2005).

At this point, considerable efforts have been directed towards solving the aforementioned problems by improving the membrane properties using different surface modification methods ranged from simple physical adsorption (Kang *et al.*, 2007; Arena *et al.*, 2011; Zhang *et al.*, 2017) to chemical bond formation (Kang *et al.*, 2007; Xu *et al.*, 2017). Recently the zwitterionic coating has gained more attention as an innovative technique for chemical surface modification of membranes (Liu *et al*., 2017). Zwitterionic materials supply more stronger binding with water molecules than hydrophilic materials via electrostatic interactions with better wetting properties because of its equal number of anionic and cationic groups (He *et al*., 2016). Therefore, zwitterionic materials compared to hydrophilic materials, leads formation of denser and tighter hydration layers. As a result, zwitterionic surface coating have demonstrated significantly increased membrane hydrophilicity and fouling resistance (Zhang *et al.*, 2013). Nguyen *et al*. (2013) modified HTI FO membrane surfaces with zwitterionic L-DOPA and L-DOPA coated membranes showed lower contact angle and 30% less fouling. The contact angle of L-DOPA coated FO membranes

were decreased from 48° to 38° (Nguyen *et al*., 2013). Also, Azari and Zou (2012) demonstrated that the organic fouling resistance of a SW30-HRXLE RO membrane was improved by L-DOPA surface modification. For the L-DOPA coated membranes, the water flux reaches 1.1 L/m^{2}hbar, almost 1.27 times higher than the permeability of pure membrane. Besides, contact angle values were also significantly improved with L-DOPA coating and decreased from 55° to 20° (Azari and Zou, 2012). The transport mechanisms with surface coating approach for enhancing membrane performance are still unknown in FO application. And to the best of our knowledge, there is no evidence of investigating the performance of zwitterionic L-DOPA modified RO membranes in FO process applications.

The objective of this study is to investigate the specific role of zwitterionic L-DOPA coating on commercial four different RO membranes and to evaluate their performances in FO process. The effects of L-DOPA modification on FO performance were examined with (BW30-LE and SW30-HR, [Dow Filmtech] and AG [GE Osmosis] and AC [Toray]) membranes. The rate of salt rejection and membrane structural properties were compared between unmodified and L-DOPA modified membranes. State-of-the-art characterization methods like as contact angle measurements, AFM, SEM and FT-IR spectroscopy were employed for all membranes used in experiments. And this paper demonstrated that L-DOPA coating is simple, stable and multifunctional modifying material to enhance significantly the membrane hydrophilicity, water flux and FO performance of commercial RO membranes. The results of the current study may provide notable understanding into the development of membrane science of FO applications.

Experimental procedure

Materials

Four different flat sheet commercial RO membranes were used in experiments and their properties were listed in Table 1.

3-(3,4-Dihydroxyphenyl)-L-alanine (L-DOPA) (MW:197 g/mole), Tris (hydroxymethyl) aminomethane buffer, NaCl and isopropyl alcohol were purchased from Sigma-Aldrich (New Zealand). All of the reagents were analytical grade. Deionized (DI) water was produced from an ultrapure water system (Millipore, USA).

Prepartion of surface modified RO membranes

To enhance the performance of BW30-LE, SW30-HR, AG and AC membranes, surface modification experiments were performed using zwitterionic L-DOPA in a flat sheet cross-flow RO membrane cell. Firstly, L-DOPA solution was dissolved in the Tris–aminomethane (10 mM, pH 8.3) buffer solution with a concentration of 2 g/L L-DOPA and mixed for 12 h. The active surfaces of membranes were coated using L-DOPA solution in cross-flow RO membrane cell (150 cm^2) for 6 h in total recycle mode of operation. After L-DOPA modification, membranes were washed three times during 1.5 h by deionized (DI) water to remove the residuals. After coating the membranes, they were soaked into 25% isopropyl alcohol solution for 15 min to remove the impurities. All membranes used in experiments were stored in DI water at +4°C (Azari and Zou, 2012).

Table 1 The properties of commercial RO membranes

Membrane	pH	Pressure (bar)	From
SW30-HR	2–11	45–15.5	Dow Filmtech
BW30-LE	2–11	95–55	Dow Filmtech
AG	2–11	44–15	GE
AC	2–11	52–15	Toray

Membrane characterizations

Morphology, topology, hydrophilicity and porosity of modified and pure RO membranes

SEM is a powerful technique to visualize morphological features of the unmodified and L-DOPA modified RO membranes. The membrane samples were fixed with an approximate size of 3 mm length and 0.5 mm width, and then coated with platinum using a JEOL JFC 1600 Autofine coater. The coated membrane was examined with A LEO 440 SEM (Leica Zeiss, Germany) at 10 Kv.

The FT-IR spectroscopy was employed for the easy identification of L-DOPA coating (Thermo Nicolet Avatar 370). Prior to the FT-IR measurements, the samples were dried in a drying oven for 15 min at 120°C.

AFM makes possible to determine surface roughness (average surface roughness (Ra), root mean square roughness [Rq] and maximum height of the profile [Rmax]). Membrane surface roughness was characterized by MultiMode 8-HR, Veeco operated in tapping mode (Model: RTESP-300). The membranes were dried overnight at 80°C to evaporate of liquid completely. The analyses were performed using a 5 × 5 μm image size. The roughness parameters of each membrane were reported as the average of at least two measurements on membranes.

The surface hydrophilicity of the membranes was determined using a contact angle meter (Attention-Theta Lite, Biolin Scientific, Finland). DI water was used to compare the hydrophilicity of the unmodified and L-DOPA modified

RO membranes. For each measurement, at least three readings from different surface locations were performed, and the reported contact angles are the average values. All of the membranes were fully dried before measuring the contact angle to water interaction.

To obtain the porosity, dry membrane was dipped in water for 24 h and then the surface of membrane coupon was dried by filter paper and immediately weighed. After that, the membranes were dried in an oven at 50°C for 24 h and weighed again. For the calculation of the average porosity of the unmodified and L-DOPA modified membranes Equation (1) (Azari and Zou, 2012) was used:

$$\text{Porosity}\,(\%) = \frac{W_w - W_d}{\rho V_m} \times 100 \quad (1)$$

where W_w and W_d are wet and dry membrane weights (g), ρ and V_m are water density (g/cm^3) and membrane coupon volume (cm^3), respectively.

Intrinsic properties of modified and pure RO membranes

A cross-flow filtration system (Sterlitech, HP4750) was used to determine the membranes' intrinsic separation properties in terms of water flux and permeability, and salt (NaCl) rejection and salt permeability. The effective area of membrane was 150 cm^2. During the experiments, the temperature was kept constant at 25 ± 5°C. The water flux was determined using DI water as a feed at 15 bar (ΔP). The water flux, J_w, of the prepared membranes were calculated using Equation (2),

$$J_w = \Delta V/(S \times \Delta t) \quad (2)$$

where J_w is the water flux (L/m^{2}h), V is the change in volume (L), S is the effective membrane area (m^2) and t is the operational time (h).

Water permeability (A) and salt permeability (B) parameters of the commercial unmodified and L-DOPA modified RO membranes were evaluated in the same lab-scale cross-flow RO test unit. The volumetric permeate rates were measured with DI water at applied pressures (ΔP) ranging from 10 to 20 bar in 5 bar increments.

The A parameter of each membrane was calculated as the average of different pressures. The calculations of A and B membrane parameters were given Equations (3) and (4);

$$A = \frac{J_w}{\Delta P} \quad (3)$$

$$B = \frac{A\,(1-R)\,(\Delta P - \Delta \pi)}{R} \quad (4)$$

where A is the water permeability, B is the salt permeability, ΔP applied pressure differences and $\Delta\pi$ osmotic pressure. Salt (NaCl) rejection, R, was also determined at 15 bar using a 20 g/L NaCl feed solution. The salt rejections were determined using Equation (5).

$$R = \left(1 - \frac{C_p}{C_f}\right) * 100 \quad (5)$$

where C_f is the salt concentration of feed solution (g/L NaCl) and C_p is the salt concentration of permeate (g/L NaCl).

FO experiments

The schematic diagram of the FO lab-scale system was illustrated in Fig. 1. It is included a membrane with active area of 48 cm^2, a digital balance, a feed tank and a draw tank, two peristaltic pumps and a conductivity meter (Fig. 1). To decrease the external concentration polarization effect on membrane, plastic mesh spacers were used. All the experiments were conducted in PRO mode, in which the active layer of the membrane faces the draw solution. Two different concentration of NaCl salt (35 and 50 g/L) was used as a draw solution and DI water was used as a feed solution. During the experiments, increase in the weights of feed solution was recorded at every 10 min using a digital balance and conductivity values were followed regularly.

The reverse salt flux, J_s (g/m^{2}h), is the salt diffusion from the draw solution to the feed solution and calculated using Equation (6) (Han *et al.*, 2012)

$$J_s = \frac{\Delta(C_f V_f)}{\Delta t S}$$

where C_f and V_f are the salt concentration and the volume of the feed solution, respectively. S is the effective membrane area (m^2) and t is the operational time (h).

Results and discussions

Membrane morphology

Morphological analysis provides a better insight for the characterization and development of the unmodified and L-DOPA modified membranes used in FO tests. The top surface images of unmodified and L-DOPA modified BW30-LE, SW30-HR, AG and AC membranes were shown in Fig. 2. These membranes were commercial polyamide (PA)-based RO membranes consisting of mechanical support to non-woven polyester fabric, polysulfone (PSF) layer and a PA selective layer (Liu *et al.*, 2008).

The unmodified SW30-HR surface layer was more porous and included large amounts of macrovoids. The unmodified BW30-LE's top layer contained fewer macrovoids and in general smaller pores (Arena *et al.*, 2011). Although unmodified SW30-HR and BW30-LE membrane surfaces have more

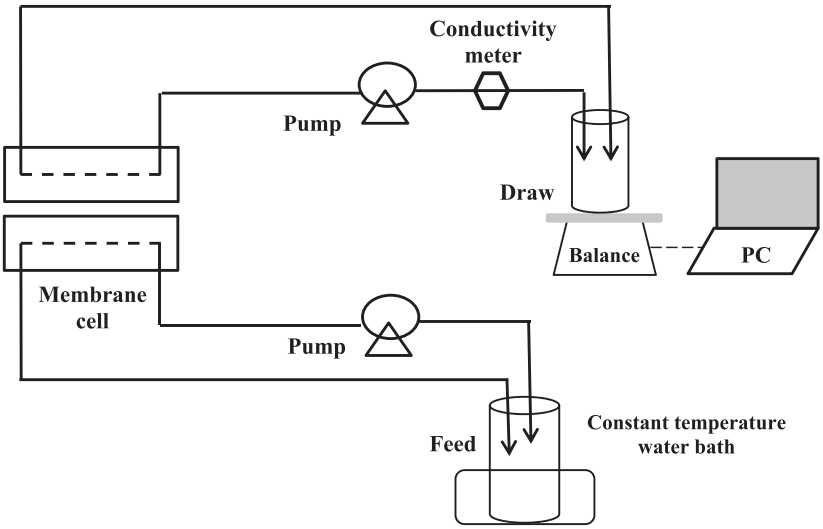

Fig. 1. Lab-scale FO module.

uniform surface without nodules, unmodified AG and AC membrane surfaces are similar with nodular morphology and completely different than BW30-LE and SW30-HR which had lots of leaf-like structures (Fig. 2). L-DOPA coating caused distinct ridge-and-valley structure of BW30-LE and SW30-HR top surface (Fig. 2). This thin L-DOPA coating was functionalized the PA selective layer which affects the water permeability and salt rejection potential of the resulting RO membrane for FO process.

Surface functional groups

The FT-IR spectra in the range of 400–4000 cm^{-1} of the unmodified and L-DOPA modified membranes were shown in Fig. 3. The PSF sublayer and the PA layer peaks could be both identified in this 400–4000 cm^{-1} region. The region between 1500 and 1800 cm^{-1} involved carbonyl groups and amide bands where the PA thin film membranes presented their specific peaks. The second characteristic peaks were evaluated between 2700 and 3700 cm^{-1} (Akin and Temelli, 2011). The top PA layer of commercial RO membranes and L-DOPA modified membranes surfaces were quite similar, such as C=O (1700 cm^{-1}), O–H (3500 cm^{-1}) or C–O–C (1000 cm^{-1}). When compared with SW30-HR membrane, BW30-LE had a few more intense peaks ~ at 3330 cm^{-1} (O–H stretching of the L-DOPA coating layer) and ~2920 cm^{-1} (C–H stretching of both the L-DOPA coating and PA layers) but a highly diluted aromatic =C–H stretching peak of the PA layer (Tang *et al.*, 2009). Xi *et al.* (2009) also observed a similar peaks for the polyethylene, poly(vinylidene fluoride) and polytetrafluoroethylene membranes coated with 0.75 wt% DOPA (Xi *et al.*, 2009).

AFM

The three-dimensional surface morphology of unmodified and L-DOPA modified membranes were analysed using tapping mode AFM and showed in Fig. 4. The coating success of L-DOPA and structural changes of membranes were clearly observed on AFM images. Although unmodified BW30-LE and SW30-HR membrane three-dimensional surfaces were quite similar with ridge-and-valley structure, AG and AC membranes have bright high peaks and nodules consistent with that in literature (Freger *et al.*, 2002). L-DOPA coating created homogeneous morphology, smoother membrane surface. It is fact that L-DOPA layer coverage on membrane surface was sufficient and the results were in agreement with literature (Maximous *et al.*, 2009).

The roughness parameters, R_q, R_a and R_{max} were summarized in Table 2. Both the maximum peak-to-valley distances and the surface roughness values were lower for the L-DOPA modified BW30-LE-LE, SW30-HR-HR and AG membranes than for the unmodified substrates, which resulted higher FO flux performance, as shown in Table 2. L-DOPA modified BW30-LE exhibited R_a value as low as 16 nm in comparison to 23 nm shown by unmodified BW30-LE and these results are in agreement with the data given in literature (Nair *et al.*, 2013). Therefore, the average roughness of the L-DOPA modified SW30-HR and AC membranes increased slightly when compared to unmodified membranes. Similarly, Zou *et al.* (2011) modified RO membrane using plasma polymerization with hydrophilic PEG and reported that, the surface roughness values increased from 61.9 to 89.3 nm of the unmodified membranes (Zou *et al.*, 2011).

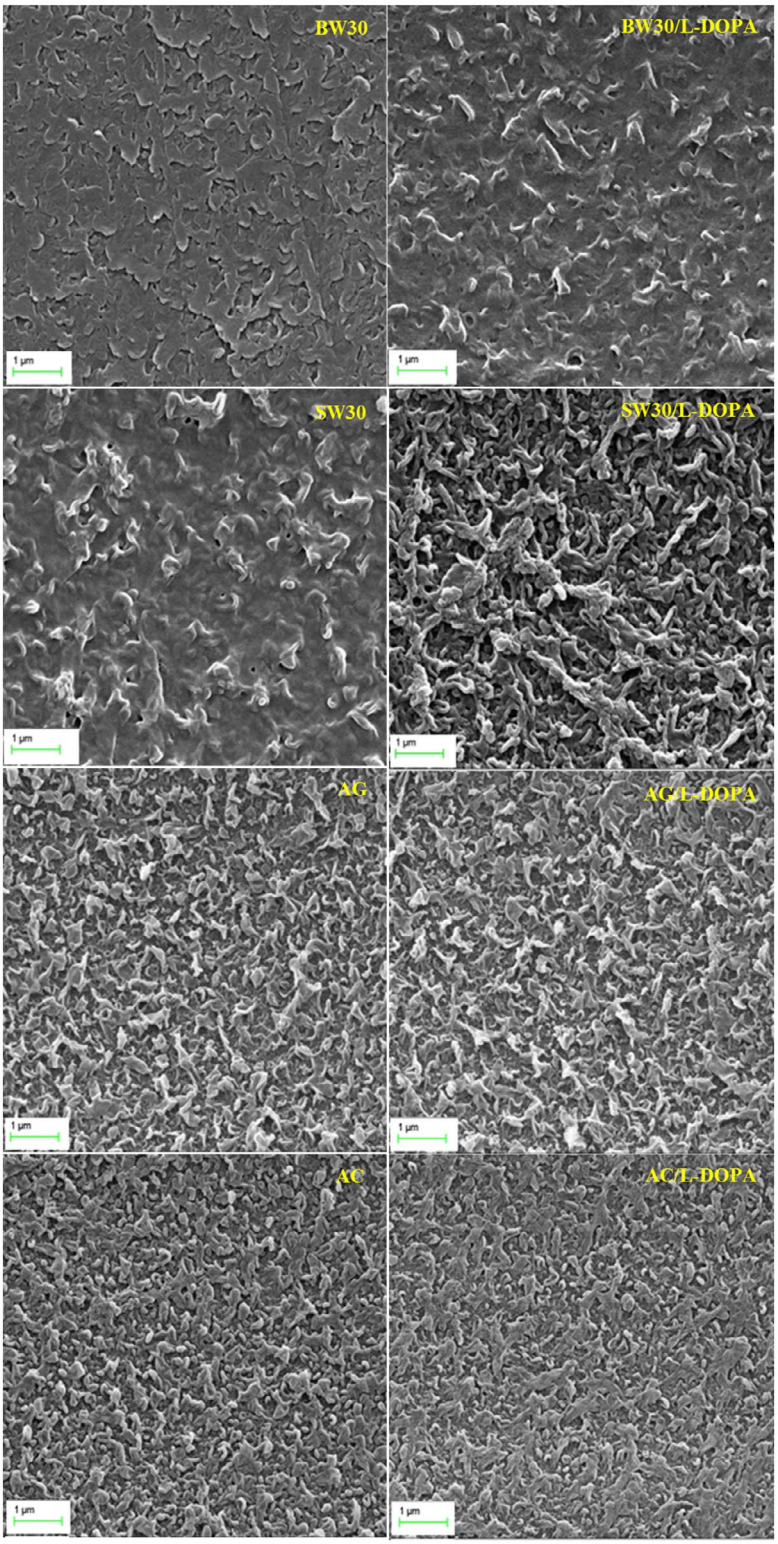

Fig. 2. SEM images of unmodified and L-DOPA modified BW30-LE, SW30-HR, AG and AC membranes surface. [Colour figure can be viewed at wileyonlinelibrary.com]

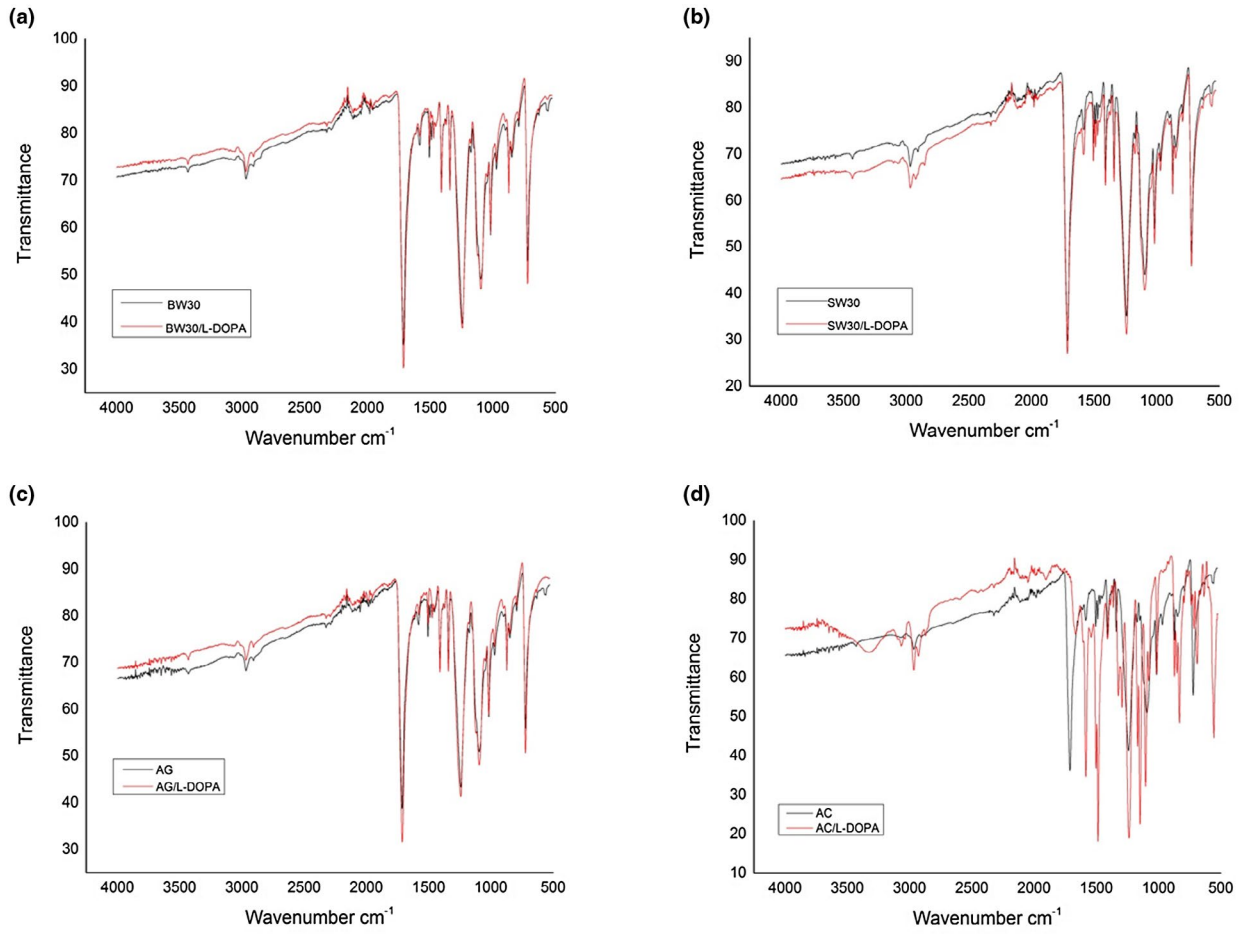

Fig. 3. FTIR spectra of unmodified and L-DOPA (2 g/L) modified membrane (a) BW30-LE, (b) SW30-HR, (c) AG and (d) AC. [Colour figure can be viewed at wileyonlinelibrary.com]

Surface hydrophilicity

Membrane contact angle is an accepted way to measure the membrane hydrophilicity which significantly affects the membrane filtration behaviour and antifouling capacity in FO experiments (Chen *et al.*, 2018). Thus, contact angle measurements were performed to investigate the membrane hydrophilicity with sessile drop method and the contact angle results of unmodified and L-DOPA modified membranes were given in Fig. 5. It was evident that the membrane hydrophilicity was improved after the L-DOPA surface modification. This can be explained by the presence of both positive and negative charged ions of zwitterionic L-DOPA, which strongly interact with water by ionic–dipole moieties. These two full charges within the L-DOPA quite increased its wettability. Meanwhile, BW30-LE and SW30-HR membranes showed more hydrophilic characteristics (Wei *et al.*, 2011) when compare to AG and AC membranes (Akin and Temelli, 2011). Also the lower contact angle of L-DOPA modified membranes may be responsible for the lower surface roughness and higher porosity and water flux (Shen and Wang, 2018).

Membrane porosity

The membrane porosity shows the empty space on the membrane structure and its related to determine the effective areas for mass transport like as membrane substrate wettability (Xiao *et al.*, 2015). The porosity values of unmodified and L-DOPA modified membranes were given in Table 3. The L-DOPA modified membrane exhibited increase in the porosity because of the influence of hydrophilic groups of L-DOPA. Also, it can be demonstrated that the porous structure is a water flow, thus and is related to the increasing of water flux of L-DOPA modified membrane. Although L-DOPA coating affected the SW30-HR porosity significantly, slight increases were

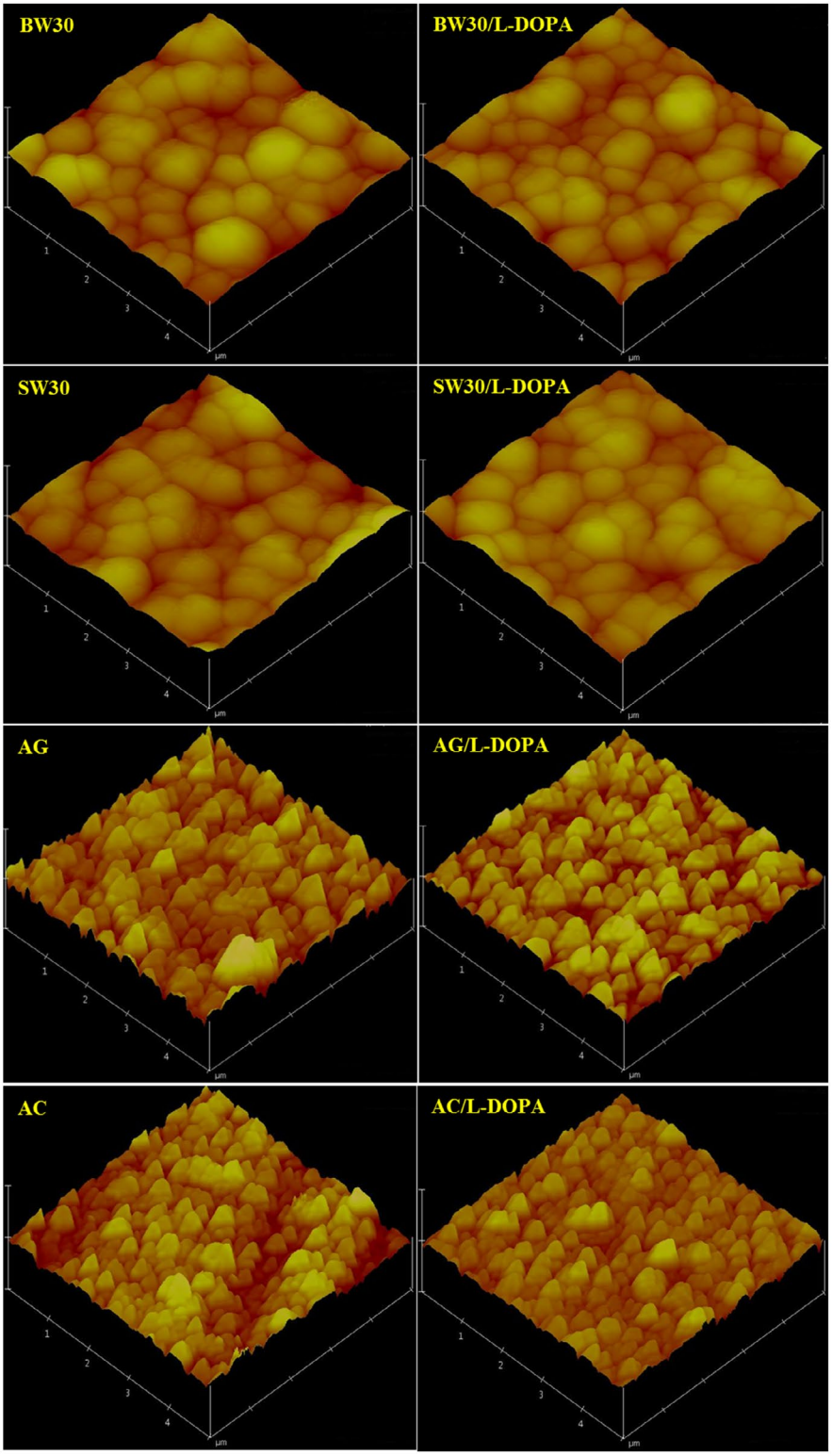

Fig. 4. AFM images of unmodified and L-DOPA modified BW30-LE, SW30-HR, AG and AC membranes. [Colour figure can be viewed at wileyonlinelibrary.com]

observed for BW30-LE, AG and AC membranes (Arena *et al.*, 2011).

Intrinsic separation properties

In order to evaluate the L-DOPA coating efficiency on the transport properties of the commercial RO membranes were investigated in RO tests at 15 bar. The steady state pure water flux results of unmodified and L-DOPA modified membranes were plotted in Fig. 6. As can be seen in Fig. 6, pure water flux values were increased with L-DOPA coating and it was most likely affected by the decline in contact angle values (Fig. 5) for all of the membranes tested. After L-DOPA modification, the increase in water fluxes ratio of AG and AC membranes were the highest with 55 and 57%, respectively. Although the L-DOPA modified AG and AC membranes showed the higher water flux increase, the highest water flux was observed for both unmodified and L-DOPA modified BW30-LE with 33.3 and 61.5 L/m^{2}h, respectively, which can be related to its high hydrophilicity, smoother surface and smaller porous structure than the other commercial RO membranes tested.

The water permeability (A) of membranes were also calculated using pure water fluxes of unmodified and L-DOPA modified membranes and membrane intrinsic separation properties were given in Table 4. Water permeability is directly affected by membrane hydrophilicity and surface roughness (Ghosh *et al.*, 2008). For the determination of salt permeability (B) and rejection (%), 20 g/L NaCl was used as a feed solution. The expected permeability-rejection trade-off was observed by more permeable membranes would be slightly lower NaCl rejection. Although lower salt rejection and higher water permeability may be observed for RO membranes because of their higher water flux at the fixed pressure used in permeation tests; the salt permeability is relatively independent of operating conditions (Cath *et al.*, 2013). After L-DOPA modification, the salt rejection was reduced with the increase in water flux and also because of higher NaCl concentration (20 g/L) of feed solution (Table 4). These results were most probably because of the L-DOPA modifications which made the membrane surface more hydrophilic and porous (Safarpour *et al.*, 2017).

Table 2 The roughness properties of unmodified and L-DOPA modified BW30-LE, SW30-HR, AG and AC membranes

Membrane	R_a (nm)	R_q (nm)	R_{max} (nm)
BW30-LE	23 ± 1.4	30 ± 0.7	190 ± 3.5
BW30-LE/L-DOPA	16 ± 1.4	20 ± 1.4	141 ± 5.6
SW30-HR	21 ± 0	27 ± 0.7	174 ± 26.1
SW30-HR/L-DOPA	22 ± 1.4	27 ± 1.4	165 ± 11.3
AG	22 ± 0	28 ± 0.7	188 ± 7.1
AG/L-DOPA	23 ± 0	29 ± 0	184 ± 19
AC	21 ± 1.4	25 ± 0.7	177 ± 4.2
AC/L-DOPA	22 ± 0.7	28 ± 0.7	203 ± 6.3

Table 3 The porosity of unmodified and L-DOPA modified BW30-LE, SW30-HR, AG and AC membranes

	BW30-LE	SW30-HR	AG	AC
Unmodified	31.5 ± 7.3	28.6 ± 0.6	18.7 ± 12.1	10.1 ± 1.8
L-DOPA modified	37.4 ± 2.4	53.7 ± 11.6	19.05 ± 0.8	12.84 ± 2.1

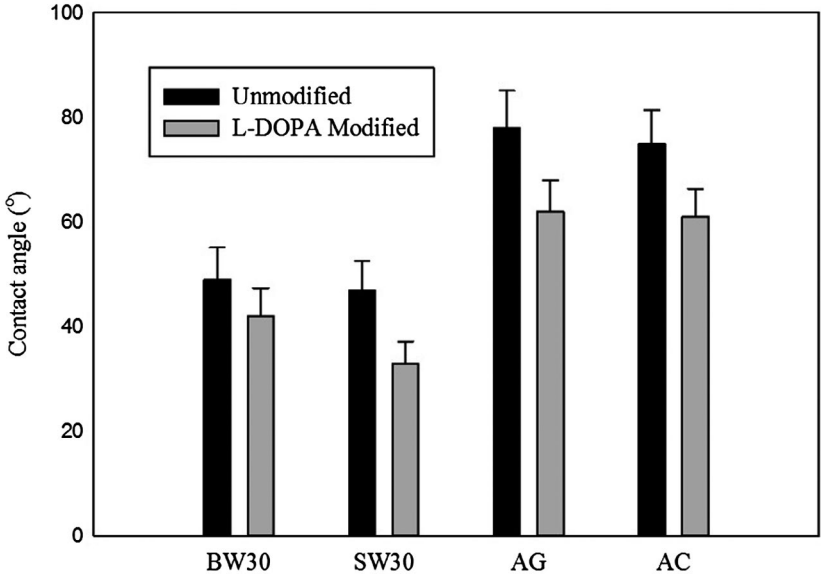

Fig. 5. Contact angles of unmodified and L-DOPA modified BW30-LE, SW30-HR, AG and AC membranes.

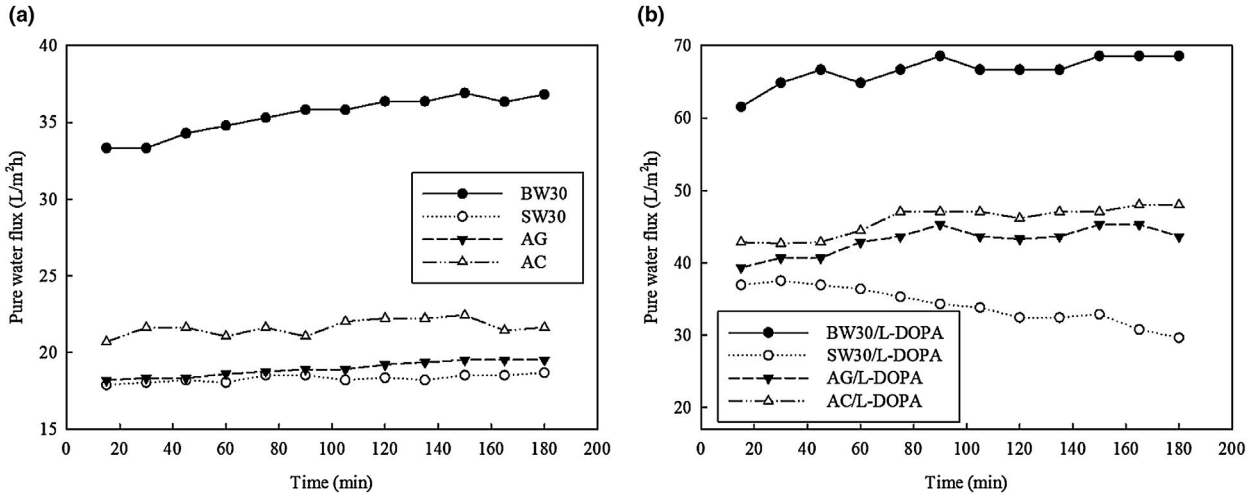

Fig. 6. Pure water flux of (a) unmodified and (b) L-DOPA modified BW30-LE, SW30-HR, AG and AC membrane at 15 bar, 25 ± 5°C.

Water and salt permeability analysis provides a clear comparison of properties that depend on the fundamental transport characteristics of the membranes (Geise *et al.*, 2011) An optimum RO/FO membrane must have some specific properties in terms of higher water permeability *A* and lower salt permeability *B*. Hence, the *B*/*A* ratio could act as a key factor for membrane performance assessment (Shokrgozar Eslah *et al.*, 2018). In general, the membrane with the smaller *B*/*A* ratio is better in reducing reverse flux during FO process. Although *A* parameter of L-DOPA modified membrane increases as a result of higher water permeability, *B* parameter decreases as a result of lower salt rejection. L-DOPA modified BW30-LE membrane showed excellent properties with 3.8 L/m²hbar water permeability and 0.83 L/m²h salt permeability within the membranes tested. This value was an order of magnitude higher than commercial brackish water RO membranes, but the other reverse osmosis membranes were similar intrinsic properties (Akin and Temelli, 2011). For all commercial L-DOPA modified RO membranes were comparable with FO membranes in the literature and even showed higher water permeability and better NaCl rejection (Wang *et al.*, 2010a). Commercial HTI membrane had low water permeability with 0.6 L/m²hbar *A* value and high salt rejection with 0.4 L/m²h *B* value (kuang *et al.*, 2016). Similarly *A* and *B* parameters of cellulose triacetate (CTA) membrane were determined as 0.80 and 0.6 L/m²h, respectively (Tang *et al.*, 2010).

Table 4 The pure water flux (15 bar), salt rejection and *A* and *B* parameters of unmodified and L-DOPA modified BW30-LE, SW30-HR, AG and AC membranes

Membrane	J_w (L/m²h)	*A* (L/m²hbar)	*R* (%)	*B* (L/m²h)
BW30-LE	33.3	2.3	81	0.83
BW30-LE/L-DOPA	61.5	3.8	72	0.75
SW30-HR	19.5	1.3	77	0.19
SW30-HR/L-DOPA	30.8	2.3	76	0.36
AG	20	1.6	78	0.22
AG/L-DOPA	45	2.8	75	0.46
AC	21.4	1.4	80	0.17
AC/L-DOPA	50	3.5	71	0.71

Forward osmosis

FO performance of the unmodified and L-DOPA modified RO membranes were tested using DI water as the feed and two different concentrations of NaCl solutions (35 and 50 g/L) as the draw solution. The water flux values were demonstrated as a function of the time in orientation of active layer facing draw solution (AL-DS) in Fig. 7. L-DOPA modified BW30-LE had more poor FO performance despite of its notable water permeability (*A* = 3.8 L/m²hbar). The FO flux is related with water permeability and the osmotic pressure gradient across the membrane. Since the highest *A* value of L-DOPA modified BW30-LE membrane compared to L-DOPA modified SW30-HR membrane, the FO flux increase was expected (Chen *et al.*, 2017). However, the osmotic pressure gradient can also depending on the concentration polarization in the AL-DS mode, internal concentration polarization occurred in the membrane active layer as a result of water try to flow from the draw to the feed side. Because of higher degree of internal concentration polarization cause lower osmotic pressure gradient that leads to a lower FO flux (McCutcheon and Elimelech, 2006). On the other hand; the L-DOPA modified SW30-HR membrane had the highest FO water fluxes when compared to all L-DOPA

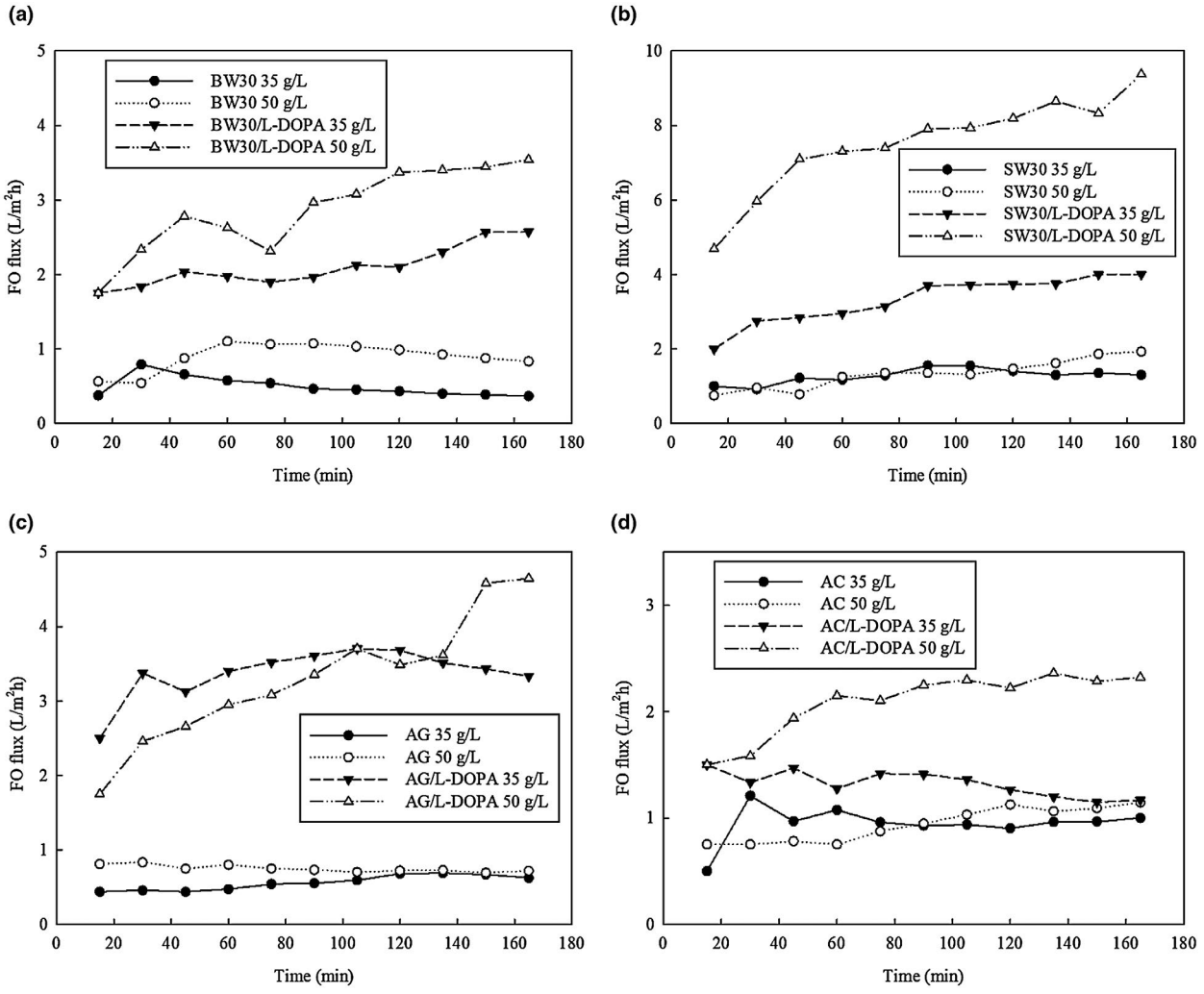

Fig. 7. FO performance of unmodified and L-DOPA modified (a) BW30-LE, (b) SW30-HR, (c) AG and (d) AC membranes.

modified membranes with a 50 g/L NaCl draw solution. FO flux values of SW30-HR membrane was increased from 1.8 to 9.38 L/m²h dramatically with the increase in the draw solution salt concentration to 50 g/L with L-DOPA modification. In fact that the highest FO flux exhibited less internal concentration polarization because of its higher porosity of the L-DOPA modified SW30-HR membrane. As an osmotically driven membrane process, the draw solution NaCl concentration impacts FO performance directly (Lay *et al.*, 2010; Wang *et al.*, 2010b). The beneficial effect of L-DOPA is well-known for membrane with the improved hydrophilicity and mass transfer (Schwinge *et al.*, 2004). But also the current study demonstrates more significant improvements on membrane for the FO performance.

The reverse salt flux values of unmodified and L-DOPA modified membranes as a function of the draw solution in PRO mode were demonstrated in Fig. 8. The reverse salt fluxes increased with the increase in draw solution concentration in accordance of osmotic pressure differences for all membrane tested and this observation values were similar with the literature (Han *et al.*, 2012). Since FO occurs as an osmotic pressure difference between the feed and draw solution, both water flux and reverse salt flux were increased naturally (Oh *et al.*, 2018). Overall, the SW30-HR membranes were the outperformed RO membranes with higher FO flux and lower reverse salt flux (Huang and McCutcheon, 2014). However, the FO flux was dramatically increased with the L-DOPA coating of RO membranes tested and any significant change was not observed in reverse salt fluxes. In addition, with the L-DOPA coating, AG and AC membranes showed increasing reverse salt fluxes and it can be explained by water flux increasing without

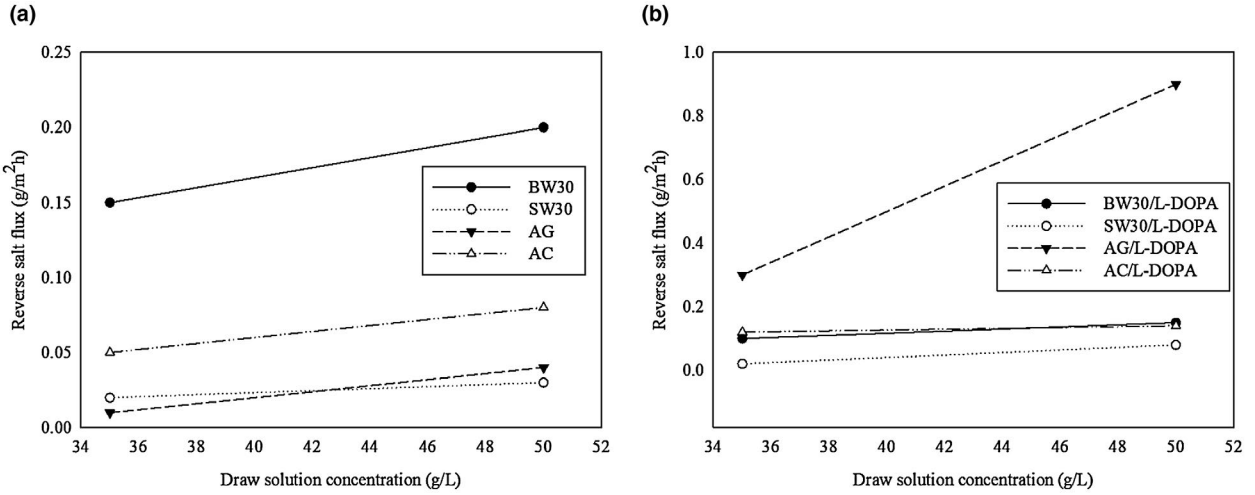

Fig. 8. Reverse salt flux of unmodified and L-DOPA modified (a) BW30-LE, (b) SW30-HR, (c) AG and (d) AC membranes.

significant smoothness and porous membrane characteristics.

Conclusions

(1) Zwitterionic L-DOPA carrying amine and hydroxyl groups were applied with a simple and easy modification process to the four different commercial polyamide RO membranes (SW30-HR, BW 30, AG and AC). The presence of hydroxyl groups on membrane surface improves the hydrophilicity of the resultant modified membranes. L-DOPA modification increased the hydrophilicity, porosity and smoothness of all the membranes tested and improved the hydraulic permeability. Membrane intrinsic separation properties were improved with L-DOPA incorporation and resulted as the enhancement in water permeability.

(2) FO performance evaluations showed that zwitterionic L-DOPA modification and the increase in draw solution concentration enhanced the FO fluxes of all membranes tested. L-DOPA modified SW30-HR membrane showed superior FO flux with 9.38 L/m^{2}h at 50 g/L NaCl draw solution. Although the L-DOPA modified BW30-LE membrane exhibited higher hydrophilicity and lower surface roughness with the 46° and 16 nm, respectively, it showed lower FO performance compared with L-DOPA modified SW30-HR membrane with 3.8 L/m^{2}hbar water permeability, 0.83 L/m^{2}h salt permeability.

(3) This study provides an insight into the exploration of modification of RO membranes with high FO performance and may be treated as a simple post manufacturing process and also extend the use of these membranes in FO technology.

Acknowledgements

The authors gratefully acknowledge the Scientific and Technological Research Council of Turkey for financial support (Project No.: 115Y617).

References

Achilli, A., Cath, T.Y. and Childress, A.E. (2009) Power generation with pressure retarded osmosis: an experimental and theoretical investigation. *Journal of Membrane Science*, **343**(1), 42–52.

Akin, O. and Temelli, F. (2011) Probing the hydrophobicity of commercial reverse osmosis membranes produced by interfacial polymerization using contact angle, XPS, FTIR, FE-SEM and AFM. *Desalination*, **278**(1), 387–396.

Arena, J.T., McCloskey, B., Freeman, B.D. and McCutcheon, J.R. (2011) Surface modification of thin film composite membrane support layers with polydopamine: enabling use of reverse osmosis membranes in pressure retarded osmosis. *Journal of Membrane Science*, **375**(1), 55–62.

Azari, S. and Zou, L. (2012) Using zwitterionic amino acid l-DOPA to modify the surface of thin film composite polyamide reverse osmosis membranes to increase their fouling resistance. *Journal of Membrane Science*, **401–402**(Supplement C), 68–75.

Boo, C., Elimelech, M. and Hong, S. (2013) Fouling control in a forward osmosis process integrating seawater desalination and wastewater reclamation. *Journal of Membrane Science*, **444**(Supplement C), 148–156.

Cath, T.Y., Elimelech, M., McCutcheon, J.R., McGinnis, R.L., Achilli, A., Anastasio, D., *et al*. (2013) Standard methodology for evaluating membrane performance in osmotically driven membrane processes. *Desalination*, **312**, 31–38.

Chen, G., Liu, R., Shon, H.K., Wang, Y., Song, J., Li, X.-M. and He, T. (2017) Open porous hydrophilic supported thin-film composite forward osmosis membrane via co-casting for treatment of high-salinity wastewater. *Desalination*, **405**, 76–84.

Chen, L.Y., Wu, L.P., Zhang, H.L., Gao, Y.B. and Gai, J.G. (2018) Tris (hydroxymethyl) aminomethane polyamide thin-film-composite antifouling reverse osmosis membrane. *Journal of Applied Polymer Science*, **135**(8):45891.

Chowdhury, M.R., Ren, J., Reimund, K. and McCutcheon, J. R. (2017) A hybrid dead-end/cross-flow forward osmosis system for evaluating osmotic flux performance at high recovery of produced water. *Desalination*, **421**(Supplement C), 127–134.

Freger, V., Gilron, J. and Belfer, S. (2002) TFC polyamide membranes modified by grafting of hydrophilic polymers: an FT-IR/AFM/TEM study. *Journal of Membrane Science*, **209**(1), 283–292.

Ge, Q., Amy, G.L. and Chung, T.-S. (2017) Forward osmosis for oily wastewater reclamation: multi-charged oxalic acid complexes as draw solutes. *Water Research*, **122**(Supplement C), 580–590.

Geise, G.M., Park, H.B., Sagle, A.C., Freeman, B.D. and McGrath, J.E. (2011) Water permeability and water/salt selectivity tradeoff in polymers for desalination. *Journal of Membrane Science*, **369**(1), 130–138.

Ghosh, A.K., Jeong, B.-H., Huang, X. and Hoek, E.M.V. (2008) Impacts of reaction and curing conditions on polyamide composite reverse osmosis membrane properties. *Journal of Membrane Science*, **311**(1), 34–45.

Goosen, M.F.A., Sablani, S.S., Al-Hinai, H., Al-Obeidani, S., Al-Belushi, R. and Jackson, D. (2005) Fouling of reverse osmosis and ultrafiltration membranes: a critical review. *Separation Science and Technology*, **39**(10), 2261–2297.

Han, G., Zhang, S., Li, X., Widjojo, N. and Chung, T.-S. (2012) Thin film composite forward osmosis membranes based on polydopamine modified polysulfone substrates with enhancements in both water flux and salt rejection. *Chemical Engineering Science*, **80**, 219–231.

Hancock, N.T. and Cath, T.Y. (2009) Solute coupled diffusion in osmotically driven membrane processes. *Environmental Science & Technology*, **43**(17), 6769–6775.

He, M., Gao, K., Zhou, L., Jiao, Z., Wu, M., Cao, J., *et al.* (2016) Zwitterionic materials for antifouling membrane surface construction. *Acta Biomaterialia*, **40**, 142–152.

Huang, L. and McCutcheon, J.R. (2014) Hydrophilic nylon 6,6 nanofibers supported thin film composite membranes for engineered osmosis. *Journal of Membrane Science*, **457**, 162–169.

Jin, X., Shan, J., Wang, C., Wei, J. and Tang, C.Y. (2012) Rejection of pharmaceuticals by forward osmosis membranes. *Journal of Hazardous Materials*, **227–228**(Supplement C), 55–61.

Kang, G., Liu, M., Lin, B., Cao, Y. and Yuan, Q. (2007) A novel method of surface modification on thin-film composite reverse osmosis membrane by grafting poly(ethylene glycol). *Polymer*, **48**(5), 1165–1170.

kuang, W., Liu, Z., Yu, H., Kang, G., Jie, X., Jin, Y. and Cao, Y. (2016) Investigation of internal concentration polarization reduction in forward osmosis membrane using nano-CaCO3 particles as sacrificial component. *Journal of Membrane Science*, **497**, 485–493.

Lay, W.C., Chong, T.H., Tang, C.Y., Fane, A.G., Zhang, J. and Liu, Y. (2010) Fouling propensity of forward osmosis: investigation of the slower flux decline phenomenon. *Water Science and Technology*, **61**(4), 927–936.

Lee, S., Boo, C., Elimelech, M. and Hong, S. (2010) Comparison of fouling behavior in forward osmosis (FO) and reverse osmosis (RO). *Journal of Membrane Science*, **365**(1), 34–39.

Liu, M., Yu, S., Tao, J. and Gao, C. (2008) Preparation, structure characteristics and separation properties of thin-film composite polyamide-urethane seawater reverse osmosis membrane. *Journal of Membrane Science*, **325**(2), 947–956.

Liu, C., Lee, J., Small, C., Ma, J. and Elimelech, M. (2017) Comparison of organic fouling resistance of thin-film composite membranes modified by hydrophilic silica nanoparticles and zwitterionic polymer brushes. *Journal of Membrane Science*, **544**(Supplement C)**,** 135-142.

Lutchmiah, K, Verliefde, A, Roest, K., Rietveld, L., and Cornelissen, E. (2014) Forward osmosis for application in wastewater treatment: a review. *Water Research*, **58**(Supplement C), 179–197.

Maximous, N., Nakhla, G., Wan, W. and Wong, K. (2009) Preparation, characterization and performance of Al 2 O 3/PES membrane for wastewater filtration. *Journal of Membrane Science*, **341**(1), 67–75.

McCutcheon, J.R. and Elimelech, M. (2006) Influence of concentrative and dilutive internal concentration polarization on flux behavior in forward osmosis. *Journal of Membrane Science*, **284**(1), 237–247.

Nair, A.K., Isloor, A.M., Kumar, R. and Ismail, A.F. (2013) Antifouling and performance enhancement of polysulfone ultrafiltration membranes using CaCO3 nanoparticles. *Desalination*, **322**, 69–75.

Nguyen, Anh, Azari, Sara and Zou, Linda (2013) Coating zwitterionic amino acid l-DOPA to increase fouling resistance of forward osmosis membrane. *Desalination*, **312**(Supplement C), 82–87.

Ni, T. and Ge, Q. (2018) Highly hydrophilic thin-film composition forward osmosis (FO) membranes functionalized with aniline sulfonate/bisulfonate for desalination. *Journal of Membrane Science*, **564**, 732–741.

Oh, S.-H., Im, S.-J., Jeong, S. and Jang, A. (2018) Nanoparticle charge affects water and reverse salt fluxes in forward osmosis process. *Desalination*, **438**, 10–18.

Safarpour, M., Vatanpour, V., Khataee, A., Zarrabi, H., Gholami, P. and Yekavalangi, M.E. (2017) High flux and fouling resistant reverse osmosis membrane modified with plasma treated natural zeolite. *Desalination*, **411**, 89–100.

Schwinge, J., Neal, P., Wiley, D., Fletcher, D. and Fane, A. (2004) Spiral wound modules and spacers: review and analysis. *Journal of Membrane Science*, **242**(1–2), 129–153.

Shen, L. and Wang, Y. (2018) Efficient surface modification of thin-film composite membranes with self-catalyzed tris(2-aminoethyl)amine for forward osmosis separation. *Chemical Engineering Science*, **178**, 82–92.

Shokrgozar Eslah, S., Shokrollahzadeh, S., Moini Jazani, O. and Samimi, A. (2018) Forward osmosis water desalination: fabrication of graphene oxide-polyamide/polysulfone thin-film nanocomposite membrane with high water flux and low reverse salt diffusion. *Separation Science and Technology*, **53**(3), 573–583.

Tang, C.Y., Kwon, Y.-N. and Leckie, J.O. (2009) Effect of membrane chemistry and coating layer on physiochemical properties of thin film composite polyamide RO and NF membranes: I. FTIR and XPS characterization of polyamide and coating layer chemistry. *Desalination*, **242**(1), 149–167.

Tang, C.Y., She, Q., Lay, W.C.L., Wang, R. and Fane, A.G. (2010) Coupled effects of internal concentration polarization and fouling on flux behavior of forward osmosis membranes during humic acid filtration. *Journal of Membrane Science*, **354**(1), 123–133.

Tian, M., Wang, Y.-N., Wang, R. and Fane, A. G. (2017a) Synthesis and characterization of thin film nanocomposite forward osmosis membranes supported by silica nanoparticle incorporated nanofibrous substrate. *Desalination*, **401**(Supplement C)**,** 142-150.

Tian, M., Wang, Y.-N., Wang, R. and Fane, A.G. (2017b) Synthesis and characterization of thin film nanocomposite forward osmosis membranes supported by silica nanoparticle incorporated nanofibrous substrate. *Desalination*, **401**, 142–150.

Wang, R., Shi, L., Tang, C.Y., Chou, S., Qiu, C. and Fane, A.G. (2010a) Characterization of novel forward osmosis hollow fiber membranes. *Journal of Membrane Science*, **355**(1), 158–167.

Wang, Y., Wicaksana, F., Tang, C.Y. and Fane, A.G. (2010b) Direct microscopic observation of forward osmosis membrane fouling. *Environmental Science & Technology*, **44**(18), 7102–7109.

Wang, Y.-N., Wang, R., Li, W. and Tang, C.Y. (2017) Whey recovery using forward osmosis – Evaluating the factors limiting the flux performance. *Journal of Membrane Science*, **533**(Supplement C), 179–189.

Wei, J., Qiu, C., Tang, C.Y., Wang, R. and Fane, A.G. (2011) Synthesis and characterization of flat-sheet thin film composite forward osmosis membranes. *Journal of Membrane Science*, **372**(1), 292–302.

Xi, Z.-Y., Xu, Y.-Y., Zhu, L.-P., Wang, Y. and Zhu, B.-K. (2009) A facile method of surface modification for hydrophobic polymer membranes based on the adhesive behavior of poly(DOPA) and poly(dopamine). *Journal of Membrane Science*, **327**(1), 244–253.

Xiao, P., Nghiem, L.D., Yin, Y., Li, X.-M., Zhang, M., Chen, G., *et al*. (2015) A sacrificial-layer approach to fabricate polysulfone support for forward osmosis thin-film composite membranes with reduced internal concentration polarisation. *Journal of Membrane Science*, **481**, 106–114.

Xie, G., Xu, W. and Ge, Q. (2018) Controlling membrane ionization with bifunctional alendronates to benefit desalination through forward osmosis. *Desalination*, **447**, 147–157.

Xu, W., Chen, Q. and Ge, Q. (2017) Recent advances in forward osmosis (FO) membrane: chemical modifications on membranes for FO processes. *Desalination*, **419**, 101–116.

Yang, Y., Gao, X., Li, Z., Wang, Q., Dong, S., Wang, X., *et al*. (2018) Porous membranes in pressure-assisted forward osmosis: flux behavior and potential applications. *Journal of Industrial and Engineering Chemistry*, **60**, 160–168.

Zhang, Y., Wang, Z., Lin, W., Sun, H., Wu, L. and Chen, S. (2013) A facile method for polyamide membrane modification by poly(sulfobetaine methacrylate) to improve fouling resistance. *Journal of Membrane Science*, **446**(Supplement C), 164–170.

Zhang, X., Tian, J., Gao, S., Zhang, Z., Cui, F. and Tang, C.Y. (2017) *In situ* surface modification of thin film composite forward osmosis membranes with sulfonated poly(arylene ether sulfone) for anti-fouling in emulsified oil/water separation. *Journal of Membrane Science*, **527**(Supplement C), 26–34.

Zou, L., Vidalis, I., Steele, D., Michelmore, A., Low, S. and Verberk, J. (2011) Surface hydrophilic modification of RO membranes by plasma polymerization for low organic fouling. *Journal of Membrane Science*, **369**(1–2), 420–428.